Annals of Botany **128**: 59–71, 2021
doi: 10.1093/aob/mcab022, available online at www.academic.oup.com/aob

ANNALS OF BOTANY
Founded 1887

PART OF A FOCUS ISSUE ON ROOT BIOLOGY

Anatomical patterns of condensed tannin in fine roots of tree species from a cool-temperate forest

Izuki Endo[1,†], Miwa Kobatake[2,†], Natsuko Tanikawa[2], Tatsuro Nakaji[3], Mizue Ohashi[1] and Naoki Makita[2,*]

[1]School of Human Science and Environment, University of Hyogo, Himeji, Hyogo, 670-0092, Japan, [2]Faculty of Science, Shinshu University, Matsumoto, Nagano, 390-8621, Japan and [3]Uryu Experimental Forest, Hokkaido University, Moshiri, Hokkaido, 074-0741, Japan
**For correspondence. E-mail macky@shinshu-u.ac.jp*
[†]These authors contributed equally to this work.

Received: 18 December 2020 Returned for revision: 30 January 2021 Editorial decision: 9 February 2021 Accepted: 13 February 2021
Electronically published: 20 February 2021

• **Background and Aims** Condensed tannin (CT) is an important compound in plant biological structural defence and for tolerance of herbivory and environmental stress. However, little is known of the role and location of CT within the fine roots of woody plants. To understand the role of CT in fine roots across diverse species of woody dicot, we evaluated the localization of CT that accumulated in root tissue, and examined its relationships with the stele and cortex tissue in cross-sections of roots in 20 tree species forming different microbial symbiotic groups (ectomycorrhiza and arbuscular mycorrhiza).
• **Methods** In a cool-temperate forest in Japan, cross-sections of sampled roots in different branching order classes, namely, first order, second to third order, fourth order, and higher than fourth order (higher order), were measured in terms of the length-based ratios of stele diameter and cortex thickness to root diameter. All root samples were then stained with ρ-dimethylaminocinnamaldehyde solution and we determined the ratio of localized CT accumulation area to the root cross-section area (CT ratio).
• **Key Results** Stele ratio tended to increase with increasing root order, whereas cortex ratio either remained unchanged or decreased with increasing order in all species. The CT ratio was significantly positively correlated to the stele ratio and negatively correlated to the cortex ratio in second- to fourth-order roots across species during the shift from primary to secondary root growth. Ectomycorrhiza-associated species mostly had a higher stele ratio and lower cortex ratio than arbuscular mycorrhiza-associated species across root orders. Compared with arbuscular mycorrhiza species, there was greater accumulation of CT in response to changes in the root order of ectomycorrhiza species.
• **Conclusions** Different development patterns of the stele, cortex and CT accumulation along the transition from root tip to secondary roots could be distinguished between different mycorrhizal associations. The CT in tissues in different mycorrhizal associations could help with root protection in specific branching orders during shifts in stele and cortex development before and during cork layer formation.

Key words: Arbuscular mycorrhiza, condensed tannin, cool-temperate forest, cortex, ectomycorrhiza, fine roots, primary root, proanthocyanidin, root anatomy, secondary roots, stele.

INTRODUCTION

Fine roots (defined as roots with a diameter of <2 mm) are the most active and dynamic part of tree root systems in terms of water and nutrient uptake (Pregitzer *et al.*, 2002; McCormack *et al.*, 2015; Addo-Danso *et al.*, 2016). Assimilated carbon in plants, often allocated to below-ground parts, accounts for 10–50 % of net primary productivity in the production and turnover of fine roots (Jackson *et al.*, 1997; Gaudinski *et al.*, 2010; Finér *et al.*, 2011). This represents a major flux of ecosystem carbon into soils, where root and root-associated carbon plays a key role in soil carbon sequestration (Drake *et al.*, 2011; Tefs and Gleixner, 2012; Clemmensen *et al.*, 2013).

Fine-root systems of woody dicot plants are composed of heterogeneous root branches with primary and secondary structure development (Peterson *et al.*, 1999; Pregitzer *et al.*, 2002; Evert, 2006; Centenaro *et al.*, 2018). New roots with primary structure development, mainly in the sub-apical part, have a living cortex and are responsible mainly for water and nutrient absorption (Peterson *et al.*, 1999; Brundrett, 2002; Evert, 2006). As they mature, woody dicot roots undergo secondary structure development with radial growth, i.e. as a consequence of an increase in root diameter there is a reduction in the proportion of absorptive tissue, owing to a loss of cortex (Wells and Eissenstat, 2002; Kumar *et al.*, 2007). During root secondary growth, secondary vascular cambium and cork cambium develop in the basal part. Roots undergoing secondary structure development are of primary importance with respect to resource transportation, storage and stress tolerance (Hishi, 2007; Kumar *et al.*, 2007; Rewald *et al.*, 2012). Therefore, the

secondary structure of woody dicot roots represents a major shift in root function from absorption to transportation according to the root branching order (Wells and Eissenstat, 2002; Hishi, 2007; McCormack *et al.*, 2015).

Several studies have examined root anatomical structures according to diameter and branching order, where first-order roots are the most distal roots and second-order roots include the point where two first-order roots arise from a parent root. Secondary xylem is more common in second- and higher-order roots than in first-order roots (Eissenstat and Acher, 1999; Hishi and Takeda, 2005). Guo *et al.* (2008) revealed that the first-order roots of 23 Chinese temperate tree species exhibited greater cortex development and stele underdevelopment than higher-order roots. Determinations of species-dependent stele and cortex characteristics, based on anatomical observations of root cross-sections, can contribute to enhancing our understanding of the differences between resource acquisition and transport functions (Kong *et al.*, 2014; Mao *et al.*, 2018).

To perform these root functions in the natural field, the roots must survive. However, fine roots usually face biotic and abiotic stresses (Ramakrishna and Ravishankar, 2011; Huber and Bauerle, 2016), such as herbivores (Johnson *et al.*, 2016), pathogens, microbial symbionts, nutrient limitation (Eissenstat *et al.*, 2000), saline conditions, drought (Sánchez-Blanco *et al.*, 2014) and low temperatures (Ryyppö *et al.*, 1997). Consequently, most new small roots die, have a relatively short lifespan (95–336 d) and do not undergo secondary development (McCormack *et al.*, 2012). Wells *et al.* (2002) reported that roots with smaller diameters face greater risks of mortality, whereas thicker roots have a longer lifespan. Baddeley and Watson (2005) showed that an increase in diameter of 0.1 mm in fine roots was associated with a 16 % decrease in mortality risk. In addition, the lifespan and turnover of fine roots vary widely among species (Coleman *et al.*, 2000; Withington *et al.*, 2006; McCormack *et al.*, 2012). Considerable seasonal variation in root production and mortality among different species was observed in 12 temperate species in the eastern USA (McCormack *et al.*, 2014) and in five temperate species in north-eastern China (Gu *et al.*, 2017). Such survivorship has often been found to be species-specific in terms of growth behaviour and phenology (Steinaker *et al.*, 2010; McCormack *et al.*, 2014, 2015).

However, the characteristics of surviving roots amidst subterranean stresses remain largely unknown. The protective characteristics of developing surviving roots should be elucidated. Plants synthesize specific defensive chemicals, such as the secondary metabolites lignin and tannin, as a survival strategy (Bennett and Wallsgrove, 1994). In particular, condensed tannin (CT; also known as proanthocyanidin) binds to proteins non-specifically, thus exhibiting toxicity in some insects and herbivores and antimicrobial effects for fungi and other microorganisms (Constabel *et al.*, 2014). Condensed tannin also protects seeds, bark, leaves, the pericarp and roots from biological stresses (Ayres *et al.*, 1997; Dixon *et al.*, 2005; Barbehenn and Constabel, 2011; Constabel *et al.*, 2014) and is often found in the organ tissues of woody plants (Porter, 1994). In several species, CT concentration is induced by biotic and environmental stresses in leaves or fruits under growing conditions (Osier and Lindroth, 2001; Peters and Constabel, 2002; Ramakrishna and Ravishankar, 2011), suggesting that CT could play key role in adaptation to environmental stresses. Osawa *et al.* (2011) observed CT accumulation in seedling root cells and suggested that roots with a large accumulation area of CT could facilitate the expansion of epidermis cells in an aluminium-rich environment. The majority of studies showing a role of root CT have come from non-woody plants and laboratory experiments, and this knowledge has not yet been applied to woody roots in natural forests. Thus, efforts to better understand CT in woody root tissues can provide useful measures of a protective strategy.

On the basis of the findings of previous studies, it has been established that the high-CT tissue in tree roots may reduce palatability and attractiveness to root-feeding insects and contribute to root protection at the cellular level. However, it gives rise to a crucial question: how does the CT-accumulating tissue in roots relate to the root anatomical traits of forest tree species? To answer the question, we focused on the CT-accumulating tissue in roots as well as the root stele and cortex of forest tree species and elucidated the intra- and interspecific variation in CT and anatomical traits across orders and species of tree roots.

Another issue that needs attention is differences in the effects of tree species on optimum root development and function, which often helps our understanding of root defence and the conservation of acquired soil resources under adverse conditions (Kong *et al.* 2014; Mao *et al.* 2018). In this regard, evidence indicates that root functional traits can be categorized according to phylogenetic types (e.g. gymnosperms and angiosperms) and mycorrhizal symbiosis types [ectomycorrhizae (EM) and arbuscular mycorrhizae (AM); Guo *et al.*, 2008; Comas and Eissenstat, 2009]. Previous studies have shown that gymnosperm roots could be more resource-conservative, while angiosperm roots could be more acquisitive for water and nutrients (Liese *et al.*, 2017; Yahara *et al.*, 2019). In addition, EM species are considered more protective than AM species (Phillips *et al.*, 2013). Although root functional traits could be understood by classification with respect to both phylogenetic types and root–mycorrhizal symbiotic types, it remains unclear whether the basic patterns and variability in root anatomical development along the root branching order should exist with respect to phylogenetic types and mycorrhizal types. In addition, the relationships of anatomical traits, such as cortex and stele, with CT accumulation are generally unknown among woody plant species. To understand commonalities and differences between tree species, we used a wide variety of trees with four different combinations of phylogenetic and mycorrhizal symbiosis types (gymnosperm–EM, gymnosperm–AM, angiosperm–EM and angiosperm–AM) from a cool-temperate mixed forest in Japan. Using an integrated anatomical approach in 20 tree species, we measured the thickness of the stele and cortex, the location of CT according to branching-order-based classification, and relationships among these traits. We targeted four classes based on branching order, namely, first-order, second- to third-order, fourth-order and higher-order (higher than fourth-order), in root cross-sections. This study had the following objectives: (1) to understand the intra- and interspecific development patterns of the cortex, stele and CT accumulation in tissue according to root branching order class and tree species; (2) to determine the relationships between CT accumulation in tissues and the cortex and stele across

root branching order class and tree species; and (3) to characterize the different phylogenetic and microbial symbiosis types via a combination of root anatomical traits.

MATERIALS AND METHODS

Study area

The field study was conducted in deciduous broad-leaved and coniferous forests in Tomakomai Experimental Forest, Hokkaido University, northern Japan (42°40′ N, 141°36′ E). The study area is located on flat land, and mean annual precipitation and air temperature in the area are 1190 mm and 6.7 °C, respectively (1999–2018). Monthly mean air temperature ranges from −9.5 to 22.2 °C. The forest grows in shallow Volcanogenous Regol soils, with a depth of <0.5 m, that have developed on a 2-m-deep volcanic ash layer that accumulated after eruptions of Mt Tarumae in 1667 and 1739 (Shibata *et al.*, 1998). The mean soil electrical conductivity and pH are 115.0 μS cm^{-1} and 5.2, respectively. The dominant tree species in deciduous broad-leaved forest are *Quercus crispula* associated with *Acer pictum*, *Sorbus alnifolia* and *Tilia maximowicziana* (Hiura, 2001). In coniferous forests, one deciduous species, *Larix kaempferi* and >30 evergreen species such as *Picea glehnii*, *Abies sachalinensis* and *Chamaecyparis obtusa* were planted >40 years before this study.

We collected root samples from 20 tree species (Table 1) that covered two phylogenetic groups, namely gymnosperms and angiosperms, and two microbial symbiotic groups, namely EM and AM. The tree species were classified into four groups: gymnosperm–EM (e.g. *Picea glehnii*, *Pinus densiflora*, *Larix kaempferi*, *Abies sachalinensis* and *Picea abies*), gymnosperm–AM (e.g. *Taxus cuspidata* and *Chamaecyparis obtusa*), angiosperm–EM (e.g. *Alnus hirsuta*, *Ostrya japonica*, *Tilia maximowicziana*, *Betula platyphylla*, *Ulmus davidiana* and *Quercus crispula*) and angiosperm–AM (e.g. *Acer pictum*, *Cercidiphyllum japonicum*, *Magnolia kobus*, *Magnolia obovata*, *Cornus controversa*, *Phellodendron amurense* and *Fraxinus mandshurica*) (Smith and Read, 2008).

Root sampling

All tree root samples were collected over 3 weeks from mid-August to early September 2018. We selected three mature trees >26 years old (diameter at breast height > 15.0 cm, mean 27.3 cm) per species. We located large root systems around the target tree and traced them back to the parent trunk to identify the species within 300 cm of the trunk. For each target species, larger intact root systems were gently exposed from the soil and then sampled using pruning shears and small knives. We collected a total of 60 intact fine distal root segments from three target trees per species with first- to sixth-order branching. All root samples were placed in a cooler to retain moisture and transported to the laboratory within 1 h for anatomical study.

In the laboratory, all large root samples were gently washed with tap and distilled water to remove the attached soil. The fine-root samples (with diameters of <2.0 mm) were divided into living and dead roots based on root colour, cohesion of stele and periderm, root elasticity and morphological status. Fine roots with light colour, intact stele and periderm were usually regarded as living roots (Vogt and Persson, 1991; Hertel and Leuschner, 2002). Living roots <2 mm in diameter were classified into four classes, namely first-order, second- to third-order, fourth-order and higher-order (higher than fourth-order), using Vernier callipers and a stereomicroscope based on root-branching order according to Pregitzer *et al.* (2002), with the most distal segments classified as first-order. After first-order roots, two joint roots of the same order (xth) gave the order ($x + 1$th) to their parent roots (Mao *et al.*, 2018). The first- to third-order, fourth-order and higher-order roots were referred to diameter-based classes of <0.5, 0.5–1.0 and

Table 1. *Species information on taxonomy, mycorrhizal symbiosis, leaf habits and xylem type of 20 tree species examined in this study*

Species	Family	Taxonomy	Mycorrhizal symbiosis	Leaf habit	Xylem type
Picea glehnii	Pinaceae	Gymnosperm	EM	Evergreen	Tracheid
Picea abies	Pinaceae	Gymnosperm	EM	Evergreen	Tracheid
Pinus densiflora	Pinaceae	Gymnosperm	EM	Evergreen	Tracheid
Larix kaempferi	Pinaceae	Gymnosperm	EM	Deciduous	Tracheid
Abies sachalinensis	Pinaceae	Gymnosperm	EM	Evergreen	Tracheid
Taxus cuspidata	Taxaceae	Gymnosperm	AM	Evergreen	Tracheid
Chamaecyparis obtusa	Cupressaceae	Gymnosperm	AM	Evergreen	Tracheid
Ostrya japonica	Coryloideae	Angiosperm	EM	Deciduous	Diffuse porous
Alnus hirsuta	Betulaceae	Angiosperm	EM	Deciduous	Diffuse porous
Betula platyphylla	Betulaceae	Angiosperm	EM	Deciduous	Diffuse porous
Tilia maximowicziana	Tiliaceae	Angiosperm	EM	Deciduous	Diffuse porous
Ulmus davidiana	Ulmaceae	Angiosperm	EM	Deciduous	Rings porous
Quercus crispula	Fagaceae	Angiosperm	EM	Deciduous	Rings porous
Acer pictum	Sapindaceae	Angiosperm	AM	Deciduous	Diffuse porous
Cercidiphyllum japonicum	Cercidiphyllaceae	Angiosperm	AM	Deciduous	Diffuse porous
Magnolia kobus	Magnoliaceae	Angiosperm	AM	Deciduous	Diffuse porous
Magnolia obovata	Magnoliaceae	Angiosperm	AM	Deciduous	Diffuse porous
Cornus controversa	Cornaceae	Angiosperm	AM	Deciduous	Diffuse porous
Phellodendron amurense	Rutaceae	Angiosperm	AM	Deciduous	Rings porous
Fraxinus mandshurica	Oleaceae	Angiosperm	AM	Deciduous	Rings porous

AM, arbuscular mycorrhizae; EM, ectomycorrhizae.

1.1–2.0 mm, respectively. Because the first- to third-order roots of *P. glehnii*, *A. sachalinensis*, *P. abies*, *T. cuspidata*, *C. obtusa*, *M. kobus* and *P. amurense* had slightly thick diameter, they were categorized not as <0.5 mm but <0.6 mm. For the anatomical measurements, all roots were fixed in 2.5 % glutaraldehyde and kept at 4 °C for 2 weeks.

Histochemical analyses

For anatomical measurements, samples from the intact root system for each species were separated by branching order. Roots were excised from the root system according to root diameter class using a razor blade. The root fragments were embedded in optimal cutting temperature compound (Sakura Finetek Japan, Tokyo, Japan) and frozen at –60 °C for at least 48 h. The frozen samples were transferred to a freezer at –20 °C ~1 h before slicing. The embedded roots were sliced into cross-sections with thicknesses of 10–30 µm using a freezing microtome (CM1950, Leica, Tokyo, Japan). To avoid the destruction of internal structures during slicing, the cross-section was pasted to self-adhesive film based on Kawamoto's (2005) method. The root sections in each class were photographed under a light microscope (BX51; Olympus, Tokyo, Japan; Fig. 1, Supplementary Data Fig. 1). The anatomical traits, including root diameter (mm), cortex thickness (mm) and stele diameter (mm), of each root cross-section were measured in three directions using SPOT Advanced software (version 4.0; Diagnostic Instruments, Sterling Heights, MI, USA) and mean values of each length were calculated. We then calculated the length-based ratios (mm/mm) of cortex thickness to root diameter (cortex ratio) and stele diameter to root diameter (stele ratio). The cortex and stele ratios would reflect the relative importances of woody resource absorption and transport (Kong *et al.*, 2014).

The cross-sections were then stained with 1 % (w/v) *ρ*-dimethylaminocinnamaldehyde (DMACA) solution, which was dissolved with 3 N HCl and 50 % (v/v) methanol for 30 min to detect CT in the root sections. DMACA stains CT blue, and this colorimetric method has been used to quantify CT concentrations in plants (Li *et al.*, 1996) and visualize CT distribution in plant organs and cells (Bogs *et al.*, 2007; Osawa *et al.*, 2011). Therefore, the area stained blue by DMACA was regarded as the area of accumulation of CT tissue. The stained cross-section was placed on a glass slide and photographed under a light microscope (BX51; Olympus, Tokyo, Japan).

The position of the endodermis and presence of the cork layer were observed under a light microscope (BX51; Olympus) equipped with a WU filter (excitation, 330–385 nm; dichroic mirror, 400 nm; emission, >420 nm). The blue-stained areas were defined with respect to the following ranges of three colour attributes (colour phase, 60–150; chromaticity, 20–80; and brightness, 70–145). The stained cross-sectional areas of accumulated CT were classified with reference to a defined colour range and determined using image analysis software (WinRHIZO 2013; Regent Instruments, Quebec, Canada). The total CT ratio was calculated by dividing the blue-stained cross-sectional area by the root cross-sectional area (Supplementary Data Fig. S1).

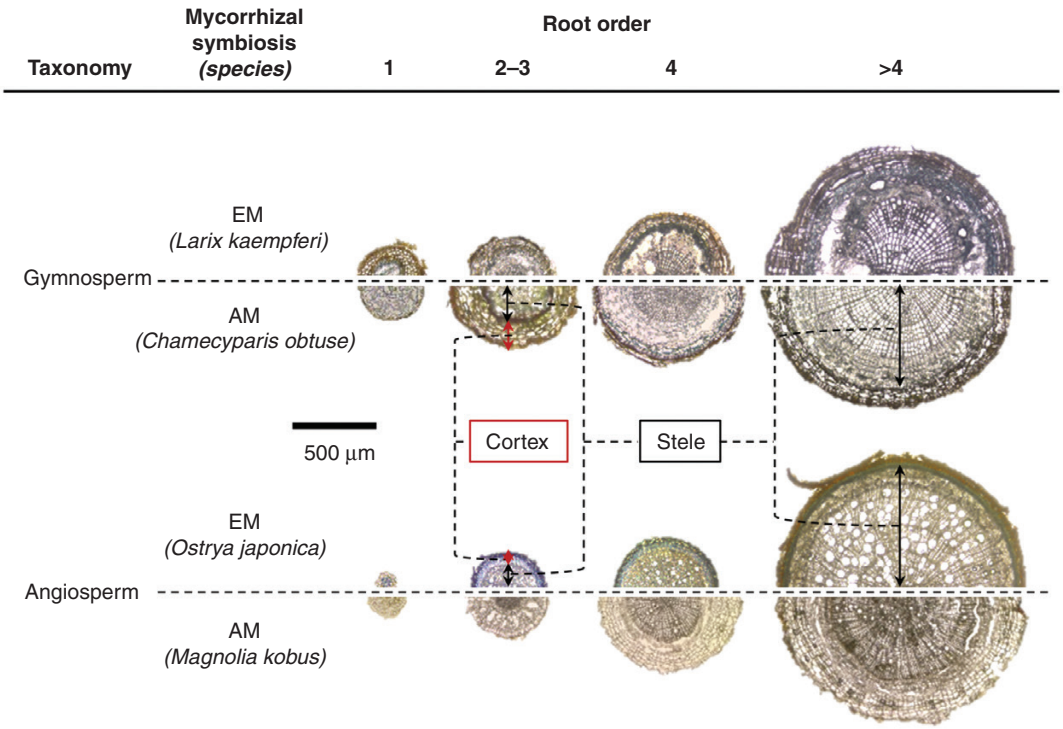

FIG. 1. Root cross-sections stained with DMACA along root branching orders in *Larix kaempferi*, *Chamaecyparis obtusa*, *Ostrya japonica* and *Magnolia kobus*. Location of CT accumulation in the root is shown by a blue colour.

Statistical analyses

For each root diameter class, the ratios of cortex thickness to root diameter, stele diameter to root diameter, and area of accumulated CT in cross-sectional samples were averaged for each target tree. For each species, means and standard errors were calculated for each root anatomical trait ($n = 3$). The effect of species on each root trait was tested using one-way analysis of variance. Tukey's HSD test ($P < 0.05$) was used to identify differences in root traits between species. To compare these differences, relative values were calculated by dividing the measured values by the mean values for each root trait. Regression analyses were performed between total CT ratio and cortex or stele ratio. Principal component analyses were conducted using the cortex, stele and total CT ratios as parameters. All statistical analyses were performed in R version 3.5.1 software (R Development Core Team, 2016).

RESULTS

Stele and cortex ratios of different classes of root branching order

The ratios of cortex thickness to root diameter (cortex ratio) and stele diameter to root diameter (stele ratio) differed significantly among root order classes in all tree species (Fig. 2, Table 2). Stele ratio tended to increase with increasing root order, whereas cortex ratio either remained unchanged or decreased with increasing order in all species (Supplementary Data Table S1). The stele and cortex ratios had similar patterns along root order across species, but the magnitudes of changes differed between species (Fig. 2). The cork layer of the roots appeared from the second- and third-order roots in several species and was often observed in higher-order roots in which the cortex was disappearing (Supplementary Data Table S2).

Total CT ratio in different classes of root branching order

Blue-stained areas were observed in 16 species, but four angiosperm–AM species (*M. kobus*, *M. obovata*, *P. amurense* and *F. mandshurica*) showed almost no colouring based on three colour attributes for evaluation criteria (Fig. 3P, Q, S, T, Supplementary Data Table S3). In the roots of the 16 species with blue colouring, we observed four patterns in the area-based ratio of CT accumulation tissue to root cross-section (total CT ratio) with increasing root order (Fig. 3, Supplementary Data Table S3). In the first type, the total CT ratio tended to decrease significantly with increasing root order, as seen in *C. obtusa* (gymnosperm–AM; Fig. 3G), *A. hirsuta* (angiosperm–EM; Fig. 3I) and *C. controversa* (angiosperm–AM; Fig. 3R). In the second type, the total CT ratio tended to increase suddenly and then gradually with increasing root order, as seen in *T. cuspidata* (gymnosperm–AM; Fig. 3F) and *B. platyphylla* (angiosperm–EM; Fig. 3J). In the third type, total CT ratio peaked in the two middle diameter classes (inverted-V shape). In this third type, peaks of total CT ratio occurred in the second- to third-order roots (*A. sachalinensis*, gymnosperm–EM; *O. japonica*, *Q. crispula*, angiosperm–EM; and *A. pictum*, angiosperm-AM; Fig. 3E, H, M, N, respectively) and in fourth-order roots (*P. glehnii*, *P. abies* and *L. kaempferi*, gymnosperm–EM; *T. maximowicziana*, and *U. davidiana*, angiosperm–EM; Fig. 3A, B, D, K, L, respectively). In the fourth pattern, the total CT ratio was constant among root orders (*P. densiflora*, gymnosperm–EM; Fig. 3C, *C. japonicum*, angiosperm–AM; Fig. 3O).

Interspecies differences in anatomical characteristics

Each root order class showed interspecies differences in anatomical characteristics (Fig. 4, Supplementary Data Table S1). Mean values for stele ratio were the lowest in first- and second- to third-order roots (Fig. 4A–D, Supplementary Data Table S1). The coefficient of variation was large in first- to third-order roots and decreased with increasing root diameter (Supplementary Data Table S1). For first-order roots, EM species mostly had stele ratio values above the mean (Fig. 4A). For second- and third-order roots, only EM species had values above the mean, except for *C. japonicum* and *A. pictum* (Fig. 4B). The stele ratio values of angiosperms were higher than those of gymnosperms (Fig. 4B, Supplementary Data Fig. S1). For fourth-order roots, EM species, four AM species (*C. japonicum*, *P. amurense*, *A. pictum* and *T. cuspidata*) had values above the mean (Fig. 4C). For higher-order roots, the stele ratio was 0.85 ± 0.08 (mean ± s.d., $n = 20$), and those of EM species and some AM species were above the mean (Fig. 4D).

Across species, mean cortex ratios were higher in first-order roots than in higher-order roots (Fig. 4E–H, Supplementary Data Table S1). For first-order roots, most species with cortex ratio values below the mean were EM species (Fig. 4E). For second- and third-order roots, the cortex ratios of angiosperm–EM species approached zero (Fig. 4F). Mostly AM species had values above the mean. For fourth-order roots, the cortex ratios of *C. japonicum* and *P. amurense* (angiosperm–AM species) approached zero or were drastically decreased (Fig. 4G). For higher-order roots, the cortex ratio in 15 species approached zero (Fig. 4H).

The mean total CT ratio was highest for fourth-order roots and lowest for higher-order roots (Fig. 4I–L, Supplementary Data Table S1). For first-order roots, five EM species had total CT ratios above the mean (Fig. 4I). Mostly angiosperm–EM species tended to have high total CT ratios. For second- to third-order and fourth-order roots, mostly EM species, especially angiosperms, had values above the mean (Fig. 4J, K). For higher-order roots, the mean total CT ratio decreased more than for fourth-order roots (Fig. 4L), and the coefficient of variation was largest for higher-order roots (Supplementary Data Table S1).

Relationship between total CT ratio and anatomical characteristics for each root order class

The relationships of total CT ratio to stele and cortex ratios varied between root diameter classes (Fig. 5). No correlation was observed for either stele or cortex ratio for first-order roots (Fig. 5A, B). For second- and third-order roots, the total CT ratio was significantly positively correlated with stele ratio (Fig. 5C, $P < 0.05$) and negatively correlated with cortex ratio

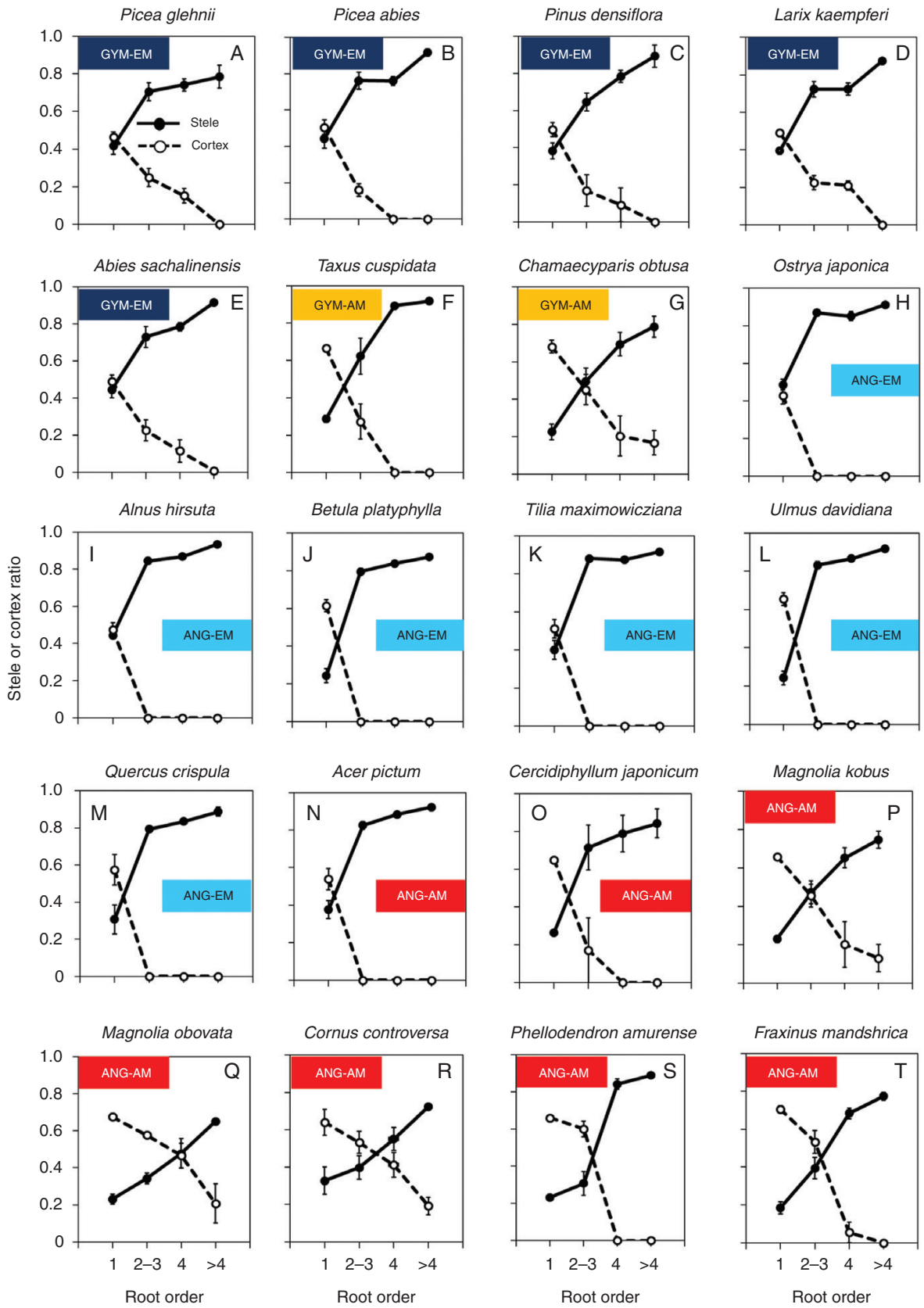

FIG. 2. Ratio of stele diameter or cortex thickness to root diameter in 20 tree species. Solid lines indicate the stele and dashed lines indicate the cortex. Values are means; error bars indicate the standard error (n = 3). ANG, angiosperm; GYM, gymnosperm.

TABLE 2. *Ratio of stele and cortex to root branching order in each root branching order class in 20 tree species*

Species	Stele: root diameter ratio					Cortex: root diameter ratio				
	Root branching order class					Root branching order class				
	1st	2nd–3rd	4th	>4th	*P*-value	1st	2nd–3rd	4th	>4th	*P*-value
Picea glehnii	0.417^{a}	0.706^{b}	0.742^{b}	0.785^{b}	0.002	0.465^{a}	0.249^{b}	0.153^{b}	0.000^{c}	<0.001
Picea abies	0.444^{a}	0.762^{b}	0.760^{b}	0.917^{b}	0.003	0.505^{a}	0.160^{b}	0.000^{c}	0.000^{c}	<0.001
Pinus densiflora	0.383^{a}	0.646^{b}	0.783^{bc}	0.893^{c}	<0.001	0.497^{a}	0.169^{b}	0.091^{b}	0.000^{b}	0.003
Larix kaempferi	0.395^{a}	0.723^{b}	0.724^{b}	0.874^{c}	<0.001	0.491^{a}	0.225^{b}	0.211^{b}	0.000^{c}	<0.001
Abies sachalinensis	0.446^{a}	0.731^{b}	0.786^{bc}	0.917^{c}	<0.001	0.491^{a}	0.226^{b}	0.116^{bc}	0.009^{c}	<0.001
Taxus cuspidata	0.287^{a}	0.623^{b}	0.893^{b}	0.917^{c}	<0.001	0.666^{a}	0.273^{b}	0.000^{c}	0.000^{c}	<0.001
Chamaecyparis obtusa	0.225^{a}	0.496^{b}	0.694^{bc}	0.787^{c}	<0.001	0.681^{a}	0.451^{ab}	0.204^{b}	0.167^{b}	0.005
Ostrya japonica	0.487^{a}	0.870^{b}	0.852^{b}	0.913^{b}	<0.001	0.428^{a}	0.000^{b}	0.000^{b}	0.000^{b}	<0.001
Alnus hirsuta	0.444^{a}	0.844^{b}	0.868^{b}	0.935^{c}	<0.001	0.473^{a}	0.000^{b}	0.000^{b}	0.000^{b}	<0.001
Betula platyphylla	0.243^{a}	0.795^{b}	0.838^{b}	0.872^{b}	<0.001	0.614^{a}	0.000^{b}	0.000^{b}	0.000^{b}	<0.001
Tilia maximowicziana	0.401^{a}	0.881^{b}	0.874^{b}	0.917^{b}	<0.001	0.512^{a}	0.000^{b}	0.000^{b}	0.000^{b}	<0.001
Ulmus davidiana	0.242^{a}	0.831^{b}	0.866^{bc}	0.919^{c}	<0.001	0.655^{a}	0.000^{b}	0.000^{b}	0.000^{b}	<0.001
Quercus crispula	0.308^{a}	0.794^{b}	0.835^{b}	0.888^{b}	<0.001	0.574^{a}	0.000^{b}	0.000^{b}	0.000^{b}	<0.001
Acer pictum	0.376^{a}	0.825^{b}	0.883^{b}	0.922^{b}	<0.001	0.538^{a}	0.000^{b}	0.000^{b}	0.000^{b}	<0.001
Cercidiphyllum japonicum	0.265^{a}	0.715^{b}	0.789^{b}	0.843^{b}	0.005	0.651^{a}	0.172^{b}	0.000^{b}	0.000^{b}	0.002
Magnolia kobus	0.231^{a}	0.473^{b}	0.653^{bc}	0.747^{c}	<0.001	0.659^{a}	0.455^{ab}	0.201^{b}	0.130^{b}	0.004
Magnolia obovata	0.230^{a}	0.343^{ab}	0.477^{bc}	0.650^{c}	<0.001	0.675^{a}	0.577^{a}	0.466^{a}	0.208^{b}	0.002
Cornus controversa	0.327^{a}	0.397^{a}	0.550^{a}	0.724^{b}	0.006	0.640^{a}	0.532^{a}	0.412^{a}	0.192^{b}	0.005
Phellodendron amurense	0.232^{a}	0.308^{a}	0.843^{b}	0.889^{b}	<0.001	0.660^{a}	0.601^{a}	0.000^{b}	0.000^{b}	<0.001
Fraxinus mandshurica	0.185^{a}	0.394^{b}	0.684^{c}	0.774^{c}	<0.001	0.705^{a}	0.534^{a}	0.055^{b}	0.000^{b}	<0.001

Different superscript letters within columns indicate significant differences between root branching orders.

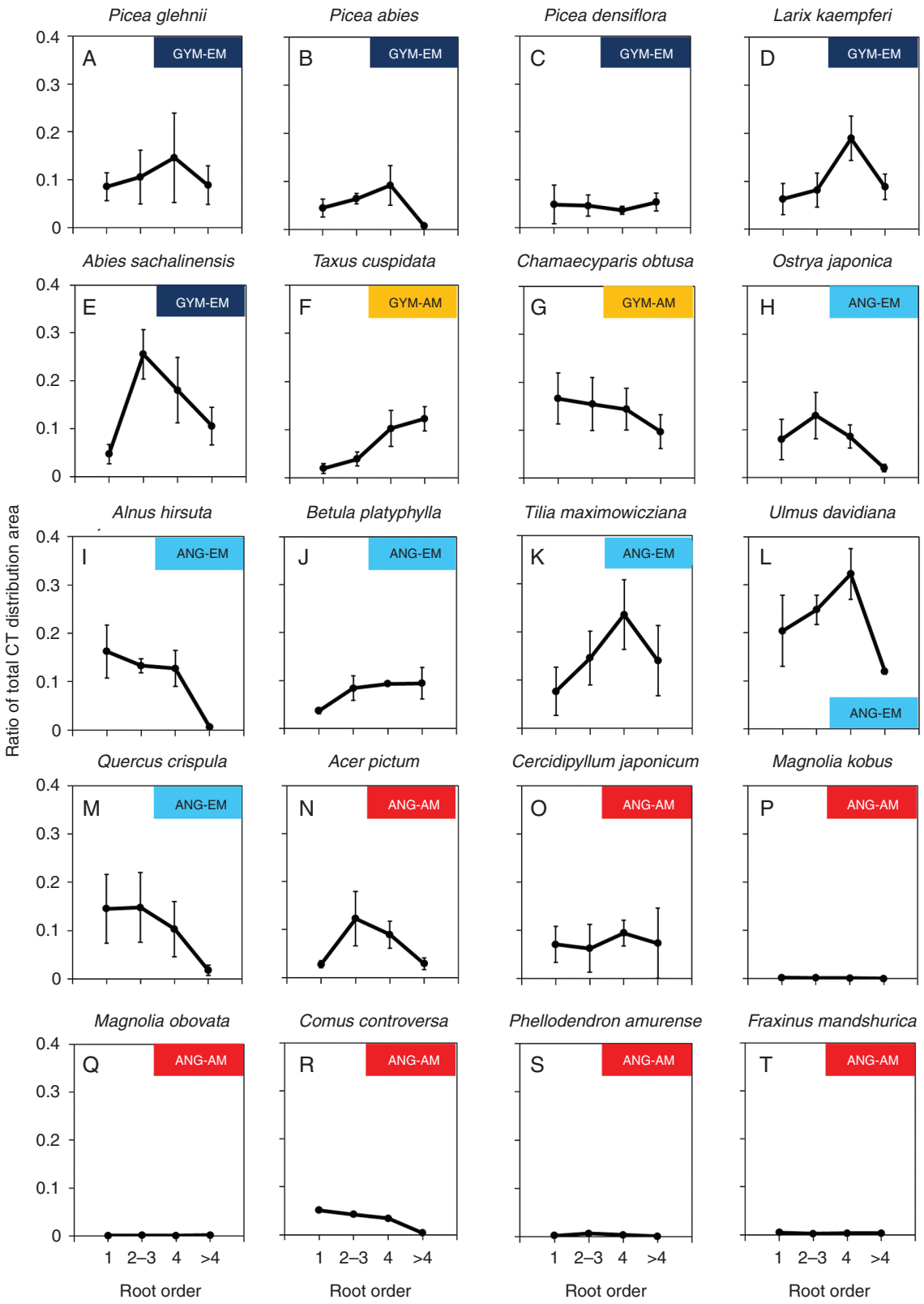

FIG. 3. Ratio of CT distribution area to root cross-sectional area in different root branching order classes in 20 tree species. Values are means; error bars indicate the standard error (n = 3). ANG, angiosperm; GYM, gymnosperm.

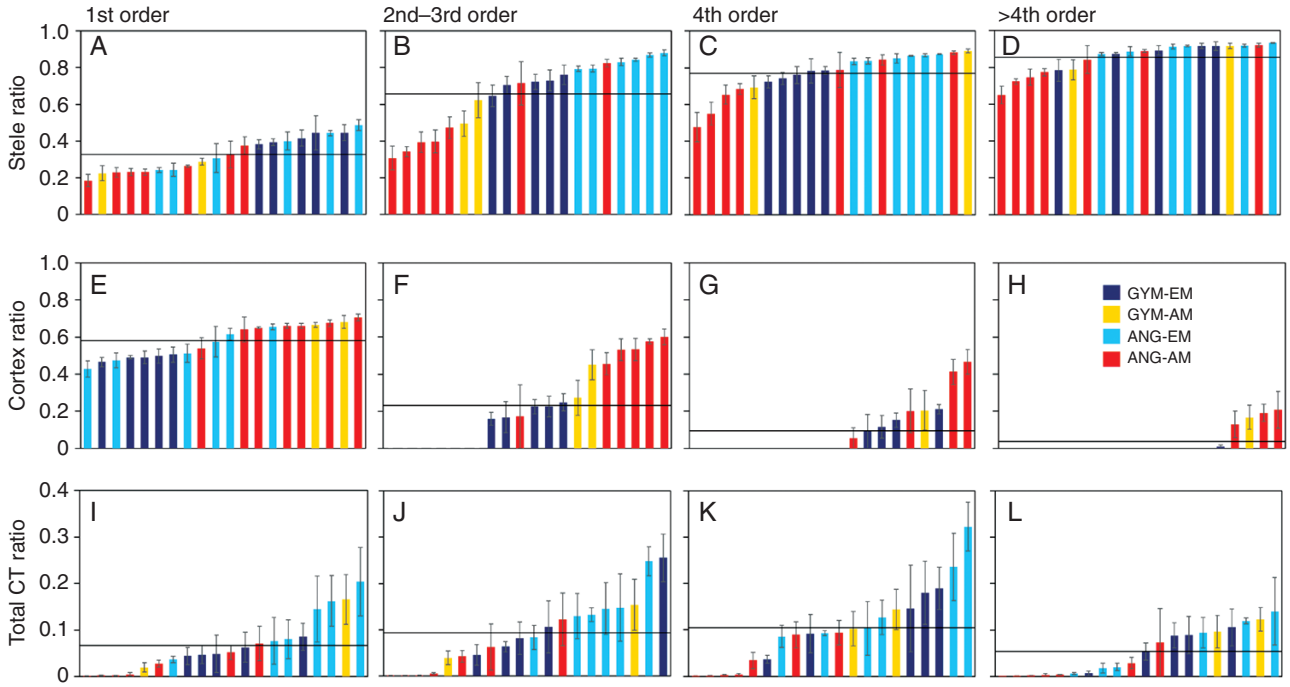

FIG. 4. Ratio of stele or cortex to root diameter and ratio of CT distribution area to root cross-sectional area from lowest to highest in 20 tree species. The horizontal line in each graph indicates the mean value. The key indicates taxonomic and microbial symbiosis groups. Values are mean ± standard error (n = 3). ANG, angiosperm; GYM, gymnosperm.

(Fig. 5D, $P < 0.05$). For fourth-order roots, total CT ratios and stele ratios were positively correlated (Fig. 5E, $P < 0.05$), but no correlation was detected between total CT ratios and cortex ratios (Fig. 5F). For higher-order roots, no correlation was observed between stele and cortex ratios (Figs 4H and 5G).

Overall variation in root stele, cortex and CT

The principal component analyses of the three anatomical characteristics of the studied species showed that the first and second principal components (factors 1 and 2) accounted for 70.06 and 29.63 % of the variation, respectively (Fig. 6). Factor 1 correlated positively with cortex ratio and negatively with stele ratio. Root diameter classes were related to factor 1, with lower-order roots tending to have higher cortex and lower stele ratios compared with those of the higher-order roots. Factor 2 correlated negatively with CT. Lower variations in total CT ratio were observed for angiosperm–AM roots along factor 2, whereas larger variations were observed for gymnosperm–EM, gymnosperm–AM and angiosperm–EM roots. In particular, the variations in EM roots increased with increasing root diameter along factor 2. Overall, there was greater variation among EM roots than among AM roots.

DISCUSSION

We assessed root cross-sectional CT distribution by examining the stele and cortex of roots of different orders below 2 mm in 20 tree species in a cool-temperate mature forest. To our knowledge, this is the first study to observe root order-dependent differences in CT via anatomical characteristics within and between forest tree species. Our results confirmed that root branching order significantly affected the patterns of anatomical traits in all species (Fig. 2; Evert, 2006; McCormack *et al.*, 2015). In lower-order roots (<0.5 mm), the primary structure and cortex were maintained without secondary growth or continuous cork layers among species (Supplementary Data Table S2). White *et al.* (2013) showed that absorptive roots, which are involved primarily in the acquisition and uptake of soil resources, have living cortical tissues with large parenchyma cells. Additionally, the absorptive roots have limited development of vascular tissue, and are maintained through interactive associations with microbial symbionts. First-order roots in our study had the highest cortex ratio among all species, but the lowest stele ratio (Figs 2 and 4, Supplementary Data Table S1). Both the cortex ratio and the stele ratio changed with increasing order in all species, which agreed with the results of previous studies (Valenzuela-Estrada *et al.*, 2009; Long *et al.*, 2013; Mao *et al.*, 2018).

Guo *et al.* (2008) showed that first-order roots exhibited cortex development and a low stele ratio, whereas higher-order roots developed cork layers with low cortex and high stele ratios in Chinese temperate tree species. Within a species, the first-order roots exhibited a high proportion of absorptive tissue, and enhanced root uptake capacitydue to a large amount of cortex tissue (Guo *et al.*, 2008). Stele development can improve transportation and stress tolerance, playing a vital role in the transition from absorption to the development of secondary xylem (Kumar *et al.*, 2007; Comas and Eissenstat, 2009). According to previous studies, most of the tree species have cortex in first- to third-order roots and secondary structure develops in fourth- and higher-order roots (such as *Acer platanoides*, McCormack *et al.*, 2015; 23 tree species, Guo *et al.*, 2008). We consider our results to be valid compared

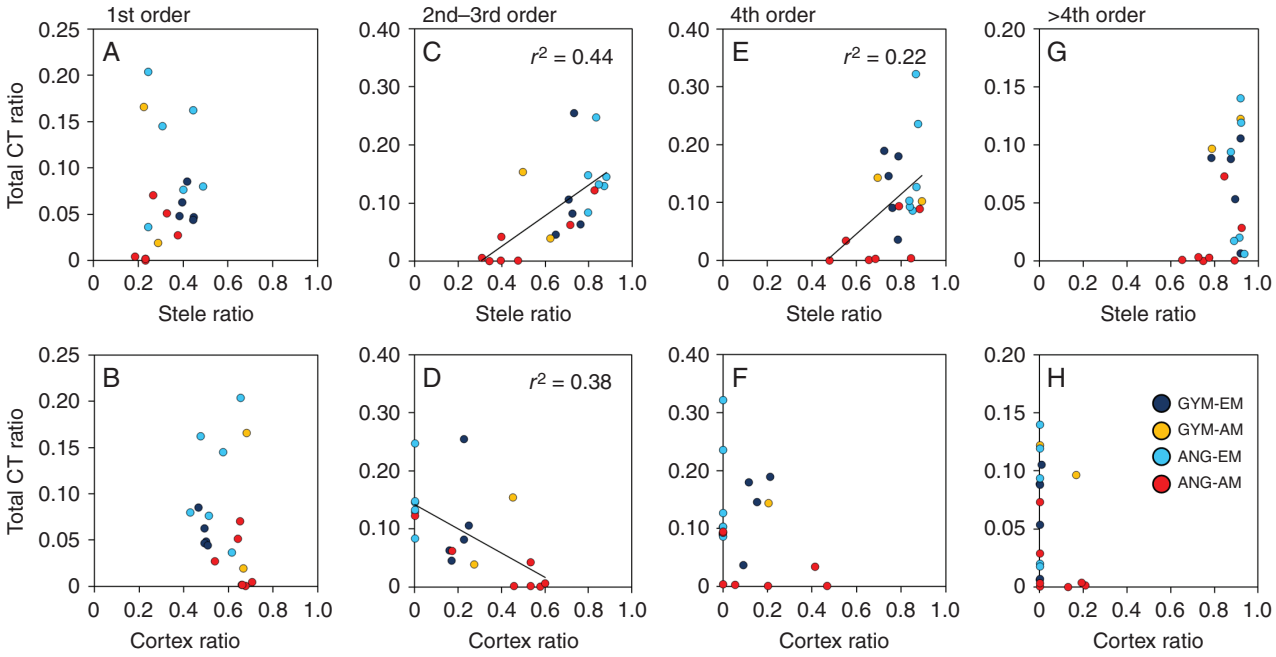

FIG. 5. Relationships between interspecific variation in CT ratio and stele or cortex ratio. (A, B) First-order roots; (C, D) second- to third-order roots; (E, F) fourth-order roots; (G, H) higher-order roots. Solid line indicates regression line for all data; $P < 0.05$. ANG, angiosperm; GYM, gymnosperm.

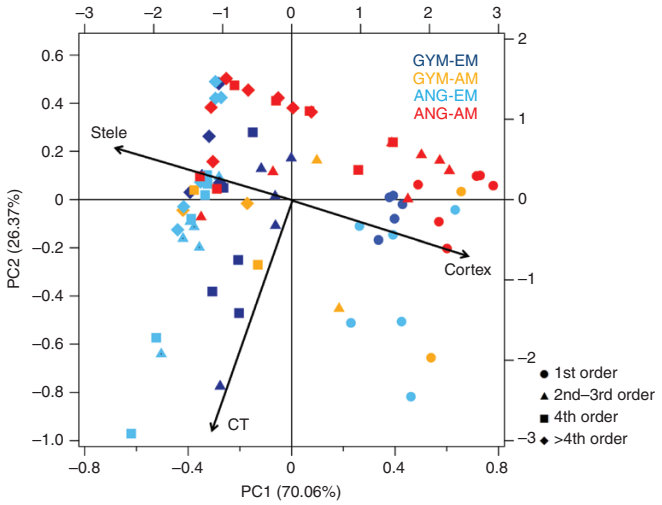

FIG. 6. Principal component analysis of anatomical root traits of 20 tree species. Tree species were classified into four groups: gymnosperm (GYM)–EM, GYM–AM, angiosperm (ANG)–EM and ANG–AM. Root sizes were classified into four groups: first-order, second- to third-order, fourth-order, and higher than fourth-order (higher-order).

with previous studies. Thus, the anatomical perspective from primary to secondary roots reflects a trade-off between resource acquisition and transportation, with higher cortex ratios favouring higher resource acquisition rates with a greater cortex area, whereas higher stele ratios favour more effective water transportation.

We found that the changes in the magnitudes of the stele and cortex ratios with increasing root order were species-dependent (Figs 2 and 4). For example, in Fig. 2 an X-shaped crossing of the stele and cortex ratios was observed in eight species, mostly of the AM type, whereas C-shaped patterns were observed in 12 species, mostly of the EM type. Histochemical observation revealed both the presence and absence of CT accumulation in the fine roots of the studied species (Fig. 3, Supplementary Data Table S3) associated with different mycorrhizal symbiosis groups. We suspect that anatomical patterns of woody dicot roots can be associated with specific strategies differently between EM and AM species based on trade-offs between resource acquisition and conservation (Guo *et al.*, 2008; Comas and Eissenstat, 2009; Yahara *et al.*, 2019). Thus, primary and secondary development of woody dicot roots through these changes in stele, cortex and total CT ratios with increasing root branching order could be classified according to the mycorrhizal symbiosis type (Fig. 4).

Mycorrhizal affiliation effects on anatomical development in our study were supported by the results of the principal component analysis. The factor 1 axis was positively correlated with cortex ratio and negatively correlated with stele ratio, suggesting a trade-off between resource acquisition and transportation with increasing root branching order (Fig. 6). High scores on the factor 1 axis were characteristic of first- to third-order EM roots and first- to fourth-order AM roots, with different anatomical growth patterns between the roots of EM and AM species in response to cortex and stele variations. The factor 2 axis was also different between EM and AM species and related to CT area in relation to changes in secondary metabolite composition and hence root chemical defence. The EM species tended to have higher CT than the AM species. This was particularly apparent in higher-order EM roots, which could provide structural support and protection. Based on our CT

distribution results, EM roots, especially higher-order roots, may be more resource-conservative than AM roots. Phillips *et al.* (2013) proposed that EM species showed root trait syndromes associated with survival and resource conservation, in contrast to AM species. Ectomycorrhizal roots are known to exhibit higher tissue density, lower specific root length and thicker diameter than roots of AM species (Valverde-Barrantes *et al.*, 2018; Bergmann *et al.*, 2020). Despite the similar cortex and stele patterns with increasing root branching order across species, CT as a chemical defensive compound could potentially explain the higher CT ratio in EM species than in AM species according to the principal component analysis (Fig. 6). There are reports that aromatic rings in CT bind to proteins and other macromolecules (Frazier *et al.*, 2010). In addition, hydroxyl groups in tannin form stable complexes with metal ions (Chin *et al.*, 2009). According to these properties, roots with higher CT could be more toxic to herbivores, fungi and bacteria than those with lower CT, and also may play a role in metal accumulation in plants (Scalbert, 1991; Chin *et al.*, 2009; Constabel *et al.*, 2014). Based on the anatomical pattern of the CT ratio and the defensive function of CT against herbivores and microbes according to previous studies, we suggest that EM roots typically exhibit considerable changes in defensive chemical properties for root protection, which are adapted to growth and structural development in woody dicot roots.

Interestingly, only in specific root orders of immature roots (i.e. second- to third-order roots), the total CT ratio increased strongly with stele ratio and decreased with cortex ratio across species (Fig. 5). The CT relationships may be attributable to the effect of root development during growth. Since woody root tips (first-order roots) are more numerous and have a higher turnover than thicker-diameter roots, they are relatively short-lived (Strand *et al.*, 2008). For *in situ* and long-term root survival and growth, both stress tolerance and defences are necessary. Our results suggest that, with the exception of some of the angiosperm–AM species, second- to third-order roots represent an initiation region for secondary growth and continuous cork development (Supplementary Data Table S2). The immature root tissues (i.e. second to third order) would be regarded as the root transition zone, located between the primary root and secondary root development regions (Kong *et al.*, 2018). To compensate for the lack of protection, they can enhance the developing stele structures by accumulating CT. Thus, the CT in the immature root tissues of the transition zone can develop with less suberization and in the absence of cork periderm and is essential for improving our understanding of shifts from primary to secondary growth related to resource transportation, storage and stress tolerance. However, our findings are limited to specific species of trees and forest sites. To extend our findings, we need to evaluate the functional roles of CT and anatomical traits in a larger number of species. We have made a significant step forward in understanding the important role of CT in terms of the linkage between development during growth and CT accumulation in root tissues using diverse tree species from different ecosystems with a range of environmental conditions.

In this study, four angiosperm–AM species (*M. kobus*, *M. obovata*, *P. amurense*, *F. mandshurica*) did not synthesize CT in fine roots. One possible defensive mechanism in these species is the development of secondary structures, such as the cork layer in woody dicot roots. In *M. kobus*, *P. amurense* and *F. mandshurica*, cortex was present in first- to third-order roots, but a cork layer developed instead of the cortex in higher-order roots (Supplementary Data Table S2). Suberin is usually deposited in the cork cell wall and plays a key role in controlling the transport of water and nutrients (Soukup *et al.*, 2004). Thus, interspecific comparisons suggested that other substances may also play such a protective role. To understand the absence of CT accumulation in specific tree species more fully, we should look for the accumulation not only of CT but also of other secondary macro- and micromolecular compounds as protective substances in fine roots, and then integrate the assessments of defensive mechanisms.

In conclusion, common anatomical traits developed from primary to secondary roots in tree species of cool-temperate forests, but the magnitudes and patterns of the stele, cortex and CT in the cross-sectional area were species-dependent. We also found a distinction between mycorrhizal groups regarding chemical protection through CT. The survival of EM roots may be helped by the conservation of resources through the assimilation of CT in tissue, while AM roots may be relatively less dependent on CT. Long-lived roots were assumed to have strong protective mechanisms because of their relatively large stele cross-sectional area and high levels of chemical defence compounds that protect them from mechanical and drought stress as well as herbivory (Kong *et al.*, 2014; Zadworny *et al.*, 2017). Especially in EM roots, the development and disappearance patterns of the stele and cortex with increasing branching order and diameter might suggest that, for the root to tolerate abiotic and biotic stresses in soil, it needs to produce CTs in root tissue as secondary chemical compounds. The cork layer formed during secondary growth is important for root tissue protection, and CT may play a protective role before and during the formation of this layer in EM roots. Root CT therefore likely contributes to enhancing plant competitiveness and vulnerabilities, including *in situ* and long-term root survival, growth and resource accumulation/transportation, by aiding in the development of stele and cortex structures in fine roots. We emphasize the need for an approach to anatomical traits and CT based on mycorrhizal symbiosis types.

SUPPLEMENTARY DATA

Supplementary data are available online at https://academic.oup.com/aob and consist of the following. Figure S1: root cross-sections stained by ρ-dimethylaminocinnamaldehyde along root branching order in 20 woody species. Table S1: mean, maximum, minimum, coefficient of variation and maximum and minimum anatomical ratios among tree species. Table S2: anatomical development of cortex and cork layer with root branching order in 20 tree species. Table S3: CT distribution in different root branching orders in 20 tree species.

FUNDING

This study was funded by a Grant-in Aid for Japan Society for the Promotion of Science Fellows (18K14488).

ACKNOWLEDGEMENTS

The authors acknowledged Prof. T. Hiura, Ms H. Yahara, Mr M. Okamoto, Ms M. Akatsuki, Mr K. Atsumi, Mr N. Watanabe, Mr R. Fujimoto, Ms A. Tamura, Ms F. Shimizu and staff members of the Tomakomai Experimental Forest, Hokkaido University, for helpful support in field and laboratory experiments. The authors also acknowledge the editor and two reviewers for giving constructive comments.

LITERATURE CITED

Addo-Danso SD, Prescott CE, Smith AR. 2016. Methods for estimating root biomass and production in forest and woodland ecosystem carbon studies: a review. *Forest Ecology and Management* **359**: 332–351.

Ayres MP, Clausen TP, MacLean SF, Redman AM, Reichardt PB. 1997. Diversity of structure and antiherbivore activity in condensed tannins. *Ecology* **78**: 1696–1712.

Baddeley JA, Watson CA. 2005. Influences of root diameter, tree age, soil depth and season on fine root survivorship in *Prunus avium*. *Plant and Soil* **276**: 15–22.

Barbehenn RV, Peter Constabel C. 2011. Tannins in plant-herbivore interactions. *Phytochemistry* **72**: 1551–1565.

Bennett RN, Wallsgrove RM. 1994. Secondary metabolites in plant defense mechanisms. *New Phytologist* **127**: 617–633.

Bergmann J, Weigelt A, van der Plas F, *et al.* 2020. The fungal collaboration gradient dominates the root economics space in plants. *Science Advances* **6**: eaba3756.

Bogs J, Jaffé FW, Takos AM, Walker AR, Robinson SP. 2007. The grapevine transcription factor VvMYBPA1 regulates proanthocyanidin synthesis during fruit development. *Plant Physiology* **143**: 1347–1361.

Brundrett MC. 2002. Coevolution of roots and mycorrhizas of land plants. *New Phytologist* **154**: 275–304.

Centenaro G, Hudek C, Zanella A, Crivellaro A. 2018. Root-soil physical and biotic interactions with a focus on tree root systems: a review. *Applied Soil Ecology* **123**: 318–327.

Chin L, Leung DW, Harry Taylor H. 2009. Lead chelation to immobilised *Symphytum officinale* L. (comfrey) root tannins. *Chemosphere* **76**: 711–715.

Clemmensen KE, Bahr A, Ovaskainen O, *et al.* 2013. Roots and associated fungi drive long-term carbon sequestration in boreal forest. *Science* **339**: 1615–1618.

Coleman MD, Dickson RE, Isebrands JG. 2000. Contrasting fine-root production, survival and soil CO2 efflux in pine and poplar plantations. *Plant and Soil* **225**: 129–139.

Comas LH, Eissenstat DM. 2009. Patterns in root trait variation among 25 co-existing North American forest species. *New Phytologist* **182**: 919–928.

Constabel CP, Yoshida K, Walker V. 2014. Diverse ecological roles of plant tannins: plant defense and beyond. *Recent Advances in Polyphenol Research* **4**: 115–142.

Dixon RA, Xie DY, Sharma SB. 2005. Proanthocyanidins – a final frontier in flavonoid research? *New Phytologist* **165**: 9–28.

Drake JE, Gallet-Budynek A, Hofmockel KS, *et al.* 2011. Increases in the flux of carbon belowground stimulate nitrogen uptake and sustain the long-term enhancement of forest productivity under elevated CO_2. *Ecology Letters* **14**: 349–357.

Eissenstat DM, Achor DS. 1999. Anatomical characteristics of roots of citrus rootstocks that vary in specific root length. *New Phytologist* **141**: 309–321.

Eissenstat DM, Wells CE, Yanai RD, Whitbeck JL. 2000. Building roots in a changing environment: implications for root longevity. *New Phytologist* **147**: 33–42.

Evert RF. 2006. *Esau's Plant anatomy: meristems, cells, and tissues of the plant body: their structure, function, and development.* Hoboken: Wiley.

Finér L, Ohashi M, Noguchi K, Hirano Y. 2011. Fine root production and turnover in forest ecosystems in relation to stand and environmental characteristics. *Forest Ecology and Management* **262**: 2008–2023.

Frazier RA, Deaville ER, Green RJ, *et al.* 2010. Interactions of tea tannins and condensed tannins with proteins. *Journal of Pharmaceutical and Biomedical Analysis* **51**: 490–495.

Gaudinski JB, Torn MS, Riley WJ, Dawson TE, Joslin JD, Majdi H. 2010. Measuring and modeling the spectrum of fine-root turnover times in three forests using isotopes, minirhizotrons, and the Radix model. *Global Biogeochemical Cycles* **24**: 1–17.

Gu JC, Wang Y, Fahey TJ, Wang ZQ. 2017. Effects of root diameter, branch order, soil depth and season of birth on fine root life span in five temperate tree species. *European Journal of Forest Research* **136**: 727–738.

Guo D, Xia M, Wei X, Chang W, Liu Y, Wang Z. 2008. Anatomical traits associated with absorption and mycorrhizal colonization are linked to root branch order in twenty-three Chinese temperate tree species. *New Phytologist* **180**: 673–683.

Hertel D, Leuschner C. 2002. A comparison of four different fine root production estimates with ecosystem carbon balance data in a *Fagus–Quercus* mixed forest. *Plant Soil* **239**: 237–251.

Hishi T. 2007. Heterogeneity of individual roots within the fine root architecture: causal links between physiological and ecosystem functions. *Journal of Forest Research* **12**: 126–133.

Hishi T, Takeda H. 2005. Life cycles of individual roots in fine root system of *Chamaecyparis obtusa* Sieb. et Zucc. *Journal of Forest Research* **10**: 181–187.

Hiura T. 2001. Stochasticity of species assemblage of canopy trees and understorey plants in a temperate secondary forest created by major disturbances. *Ecological Research* **16**: 887–893.

Huber AE, Bauerle TL. 2016. Long-distance plant signaling pathways in response to multiple stressors: the gap in knowledge. *Journal of Experimental Botany* **67**: 2063–2079.

Jackson RB, Mooney HA, Schulze ED. 1997. A global budget for fine root biomass, surface area, and nutrient contents. *Proceedings of the National Academy of Sciences of the USA* **94**: 7362–7366.

Johnson SN, Erb M, Hartley SE. 2016. Roots under attack: contrasting plant responses to below- and aboveground insect herbivory. *New Phytologist* **210**: 413–418.

Kawamoto T. 2005. Preparation and application of multipurpose fresh frozen sections from unfixed-undecalcified samples. Japanese Society for Tissue and Cell Chemistry eds., *Histocytochemistry.* Tokyo: Gakusai-Kikaku Co, Ltd, 95–107.

Kong D, Ma C, Zhang Q, *et al.* 2014. Leading dimensions in absorptive root trait variation across 96 subtropical forest species. *New Phytologist* **203**: 863–872.

Kong X, Liu G, Liu J, Ding Z. 2018. The root transition zone: a hot spot for signal crosstalk. *Trends in Plant Science* **23**: 403–409.

Kumar P, Hallgren SW, Enstone DE, Peterson CA. 2007. Root anatomy of *Pinus taeda* L.: seasonal and environmental effects on development in seedlings. *Trees – Structure and Function* **21**: 693–706.

Li YG, Tanner G, Larkin P. 1996. The DMACA-HCl protocol and the threshold proanthocyanidin content for bloat safety in forage legumes. *Journal of the Science of Food and Agriculture* **70**: 89–101.

Liese R, Alings K, Meier IC. 2017. Root branching is a leading root trait of the plant economics spectrum in temperate trees. *Frontiers in Plant Science* **8**: 315.

Long YQ, Kong DL, Chen ZX, Zeng H. 2013. Variation of the linkage of root function with root branch order. *PLoS ONE* **8**: e57153.

Mao Z, Wang Y, McCormack ML, *et al.* 2018. Mechanical traits of fine roots as a function of topology and anatomy. *Annals of Botany* **122**: 1103–1116.

McCormack ML, Adams TS, Smithwick EA, Eissenstat DM. 2012. Predicting fine root lifespan from plant functional traits in temperate trees. *New Phytologist* **195**: 823–831.

McCormack ML, Adams TS, Smithwick EA, Eissenstat DM. 2014. Variability in root production, phenology, and turnover rate among 12 temperate tree species. *Ecology* **95**: 2224–2235.

McCormack ML, Dickie IA, Eissenstat DM, *et al.* 2015. Redefining fine roots improves understanding of below-ground contributions to terrestrial biosphere processes. *New Phytologist* **207**: 505–518.

Osawa H, Endo I, Hara Y, Matsushima Y, Tange T. 2011. Transient proliferation of proanthocyanidin-accumulating cells on the epidermal apex contributes to highly aluminum-resistant root elongation in camphor tree. *Plant Physiology* **155**: 433–446.

Osier TL, Lindroth RL. 2001. Effects of genotype, nutrient availability, and defoliation on aspen phytochemistry and insect performance. *Journal of Chemical Ecology* **27**: 1289–1313.

Peters DJ, Constabel CP. 2002. Molecular analysis of herbivore-induced condensed tannin synthesis: cloning and expression of dihydroflavonol reductase from trembling aspen (*Populus tremuloides*). *Plant Journal* **32**: 701–712.

Peterson CA, Enstone DE, Taylor JH. 1999. Pine root structure and its potential significance for root function. *Plant and Soil* **217**: 205–213.

Phillips RP, Brzostek E, Midgley MG. 2013. The mycorrhizal-associated nutrient economy: a new framework for predicting carbon-nutrient couplings in temperate forests. *New Phytologist* **199**: 41–51.

Porter LJ. 1994. Flavans and proanthocyanidins. In: Harbone JB ed. *The flavonoids*. London: Chapman & Hall, 23–53.

Pregitzer KS, DeForest JL, Burton AJ, Allen MF, Ruess RW, Hendrick RL. 2002. Fine root architecture of nine North American trees. *Ecological Monographs* **72**: 293–309.

R Development Core Team. 2016. *R: A Language and Environment for Statistical Computing*. Vienna, Austria: R Foundation for Statistical Computing. http://www.R-project.org

Ramakrishna A, Ravishankar GA. 2011. Influence of abiotic stress signals on secondary metabolites in plants. *Plant Signaling & Behavior* **6**: 1720–1731.

Rewald B, Raveh E, Gendler T, Ephrath JE, Rachmilevitch S. 2012. Phenotypic plasticity and water flux rates of citrus root orders under salinity. *Journal of Experimental Botany* **63**: 2717– 2727.

Ryyppö A, Sutinen S, Mäenpää M, Vapaavuori E, Repo T. 1997. Frost damage and recovery of Scots pine seedlings at the end of the growing season. *Canadian Journal of Forest Research* **27**: 1376–1382.

Sánchez-Blanco MJ, Álvarez S, Ortuño MF, Ruiz-Sánchez MC. 2014. Root system response to drought and salinity: root distribution and water transport. In: Morte A, Varma A, eds. *Root engineering*. Berlin, Heidelberg: Springer, 325–352.

Scalbert A. 1991. Antimicrobial properties of tannins. *Phytochemistry* **30**: 3875–3883.

Shibata H, Kirikae M, Tanaka Y, Sakuma T, Hatano R. 1998. Proton budgets of forest ecosystems on Volcanogenous Regosols in Hokkaido, Northern Japan. *Water, Air, and Soil Pollution* **105**: 63–72.

Smith SE, Read DJ. 2008. *Mycorrhizal symbiosis*, 3rd edn. San Diego: Academic Press.

Soukup A, Malá J, Hrubcová M, Kálal J, Votrubová O, Cvikrová M. 2004. Differences in anatomical structure and lignin content of roots of pedunculate oak and wild cherry-tree plantlets during acclimation. *Biologia Plantarum* **48**: 481–489.

Steinaker DF, Wilson SD, Peltzer DA. 2010. Asynchronicity in root and shoot phenology in grasses and woody plants. *Global Change Biology* **16**: 2241–2251.

Strand AE, Pritchard SG, McCormack ML, Davis MA, Oren R. 2008. Irreconcilable differences: fine-root life spans and soil carbon persistence. *Science* **319**: 456–458.

Tefs C, Gleixner G. 2012. Importance of root derived carbon for soil organic matter storage in a temperate old-growth beech forest – evidence from C, N and 14C content. *Forest Ecology and Management* **263**: 131–137.

Valenzuela-Estrada LR, Richards JH, Diaz A, Eissensat DM. 2009. Patterns of nocturnal rehydration in root tissues of *Vaccinium corymbosum* L. under severe drought conditions. *Journal of Experimental Botany* **60**: 1241–1247.

Valverde-Barrantes OJ, Smemo KA, Feinstein LM, Kershner MW, Blackwood CB. 2018. Patterns in spatial distribution and root trait syndromes for ecto and arbuscular mycorrhizal temperate trees in a mixed broadleaf forest. *Oecologia* **186**: 731–741.

Vogt KA, Persson H. 1991. Measuring growth and development of roots. In: Lassoie JP, Hinckley TM, eds. *Techniques and approaches in forest tree ecophysiology.* Boca Raton: CRC Press, 477–501.

Wells CE, Eissenstat DM. 2002. Beyond the roots of young seedlings: the influence of age and order on fine root physiology. *Journal of Plant Growth Regulation* **21**: 324–334.

Wells CE, Glenn DM, Eissenstat DM. 2002. Changes in the risk of fine-root mortality with age: a case study in peach, *Prunus persica* (Rosaceae). *American Journal of Botany* **89**: 79–87.

White PJ, George TS, Gregory PJ, Bengough AG, Hallett PD, McKenzie BM. 2013. Matching roots to their environment. *Annals of Botany* **112**: 207–222.

Withington JM, Reich PB, Oleksyn J, Eissenstat DM. 2006. Comparisons of structure and life span in roots and leaves among temperate trees. *Ecological Monographs* **76**: 381–397.

Yahara H, Tanikawa N, Okamoto M, Makita N. 2019. Characterizing fine-root traits by species phylogeny and microbial symbiosis in 11 co-existing woody species. *Oecologia* **191**: 983–993.

Zadworny M, McCormack ML, Żytkowiak R, Karolewski P, Mucha J, Oleksyn J. 2017. Patterns of structural and defense investments in fine roots of Scots pine (*Pinus sylvestris* L.) across a strong temperature and latitudinal gradient in Europe. *Global Change Biology* **23**: 1218–1231.